Species-specific quorum sensing represses the chitobiose utilization locus in *Vibrio cholerae*

Catherine A. Klancher, Jane D. Newman, Alyssa S. Ball, Julia C. van Kessel, and Ankur B. Dalia*

Department of Biology, Indiana University, Bloomington, IN 47405
*Author for correspondence: ankdalia@indiana.edu

Abstract

The marine facultative pathogen *Vibrio cholerae* forms complex multicellular communities called biofilms on the shells of crustacean zooplankton in its aquatic reservoir. These shells are primarily composed of the polysaccharide chitin. *V. cholerae*-chitin interactions are critical for the growth, evolution, and waterborne transmission of cholera. This is due, in part, to chitin inducing changes in gene expression in this pathogen. Here, we sought to identify factors that influence chitin-induced expression of one locus, the chitobiose utilization operon (*chb*), which is required for the uptake and catabolism of the chitin disaccharide. Through a series of genetic screens, we identified that the master regulator of quorum sensing, HapR, is likely a direct repressor of the *chb* operon. We also found that the levels of HapR in *V. cholerae* are regulated by the ClpAP protease. Furthermore, we show that the canonical quorum sensing cascade in *V. cholerae* regulates *chb* expression in a HapR-dependent manner. Through this analysis we found that signaling via the species-specific autoinducer CAI-1, but not the inter-species autoinducer AI-2, influences *chb* expression. This phenomenon of species-specific regulation may enhance the fitness of this pathogen in its environmental niche.

Importance

In nature, bacteria live in multicellular and multispecies communities. Microbial species can sense the density and composition of their community through chemical cues using a process called quorum sensing (QS). The marine pathogen *Vibrio cholerae* forms communities on the chitinous shells of crustaceans in its aquatic reservoir, which is critical for the survival, evolution, and waterborne transmission of this pathogen. Here, we show that *V. cholerae* uses QS to regulate the expression of one locus required for *V. cholerae*-chitin interactions.

Introduction

The facultative bacterial pathogen *Vibrio cholerae* is the causative agent of the diarrheal disease cholera and natively resides in the aquatic environment. In this niche, *V. cholerae* forms multicellular communities on biotic and abiotic chitinous surfaces, like the shells of crustaceans or marine snow (1). Chitin is a polysaccharide made up of β-1,4 linked *N*-acetylglucosamine (GlcNAc) and serves as a major nutrient source for *V. cholerae* in the marine environment. The

ability of *V. cholerae* to form chitin biofilms is critical for the waterborne transmission of *V.* cholerae (2, 3). As chitin is the most abundant biopolymer in the ocean, the ability of *Vibrio* species to break down and utilize this highly insoluble polysaccharide also serves an important role in global nitrogen and carbon recycling (1). Chitin induces genetic programs in many *Vibrio* species that may increase their fitness in the environment, such as the chitin utilization program and natural competence (4, 5).

The chitin utilization program in *V. cholerae* is robust and highly regulated. To study this program, most studies employ the chitobiose utilization operon (*chb*), which is required for the uptake and catabolism of the chitin disaccharide and is highly induced in the presence of chitin oligosaccharides (4). Presently, there are several regulators of this program that have been identified. ChiS is the master regulator of the chitin utilization program in *V. cholerae*, and we have recently shown this protein is a direct transcriptional activator required for induction of the *chb* locus (6, 7). Previous work has shown that carbon catabolite repression (CCR) can also play a role in regulating chitin responsive phenotypes including ChiS-dependent induction of *chb* and natural competence (8, 9). In addition, our group has previously found that the cell division licensing factor SlmA plays an essential role in activating *chb* expression (10). Tight regulation via these diverse signaling systems may act to ensure that the chitin utilization program is only expressed under conditions in which it will provide a competitive advantage.

Here, through a number of genetic screens and complementary molecular methods we show that quorum sensing is an additional regulatory system that tunes expression of a chitin utilization locus in *V. cholerae*.

Results

ClpA is identified in an unbiased screen for activators of P_{chb}

To identify additional genes required for activation of the *chb* locus, we conducted a transposon mutant screen. This was carried out in a strain containing a P_{chb}-*lacZ* transcriptional reporter. As shown previously, induction of P_{chb} is dependent on the activity of the master regulator ChiS (4, 7). In the absence of chitin, ChiS activity is repressed by CBP. In the presence of chitin, CBP repression of ChiS is relieved, which allows for ChiS-dependent activation of P_{chb}. ChiS can also be activated genetically in the absence of chitin by deleting *cbp* (7, 10). As chitin oligomers are prohibitively expensive, a Δ*cbp* mutation was used to induce ChiS-dependent P_{chb}-*lacZ* expression in our genetic screen exactly as previously described (10). So, the starting genotype for our screen was a strain containing P_{chb}-*lacZ* and a Δ*cbp* mutation. This strain formed blue colonies on X-gal containing plates and we screened for white colonies to identify putative activators that act downstream of ChiS to contribute to P_{chb} induction.

One gene identified in this genetic screen was *clpA*. To study the effect of ClpA on P_{chb} activity moving forward, we utilized a previously described P_{chb}-GFP reporter (7, 10). Using this reporter, we found that a Δ*clpA* mutation resulted in a

93 ~3-fold decrease in P_{chb} expression relative to the parent (**Fig. 1**). ClpA is a
94 AAA+ unfoldase that recognizes protein substrates, unfolds them, and feeds
95 them into the ClpP protease where they are degraded (11). If ClpA was exhibiting
96 its effect on P_{chb} expression as a part of the ClpAP machine, we hypothesized
97 that a Δ*clpP* mutation should phenocopy a Δ*clpA* mutation. Indeed, Δ*clpP* and
98 Δ*clpP* Δ*clpA* strains phenocopied a Δ*clpA* mutant for P_{chb} expression (**Fig. 1**).
99 These results suggest that loss of the ClpAP protease decreases P_{chb}
100 expression. As ClpAP normally degrades proteins, we hypothesized that ClpAP
101 may indirectly promote activation of P_{chb} by degrading a repressor of the *chb*
102 locus.
103
104 *HapR is a repressor of P_{chb} that is degraded by ClpAP*
105 To identify a putative repressor of P_{chb} that is targeted by ClpAP for degradation,
106 we conducted a counter-screen using the P_{chb}-*lacZ* reporter. For the counter-
107 screen, the parent strain had both Δ*cbp* and Δ*clpA* mutations. This mutant is
108 white on X-gal plates because P_{chb}-*lacZ* is poorly expressed; inactivation of the
109 putative repressor in this strain should result in restoration of P_{chb}-*lacZ*
110 expression and yield a blue colony phenotype. In this counter-screen, we
111 identified *hapR*. A Δ*hapR* mutation restored P_{chb} expression in the Δ*clpA* mutant
112 background (**Fig. 1**). In fact, a Δ*hapR* mutation allowed for higher P_{chb} expression
113 than the parent strain. This suggests that HapR also represses P_{chb} expression
114 when ClpAP is intact; and that ClpAP does not degrade the entire pool of HapR
115 in the cell (**Fig. 1**). Importantly, the level of P_{chb} expression observed in the
116 Δ*hapR* Δ*clpA* mutant phenocopied the Δ*hapR* strain (**Fig. 1**). This epistasis
117 between *clpA* and *hapR* suggests that they are involved in the same pathway for
118 regulating P_{chb} expression.
119
120 We hypothesized that the reason P_{chb} expression is decreased in *clpAP* mutants
121 was due to increased HapR protein levels. Western blotting in these
122 backgrounds revealed that HapR levels were, indeed, increased in strains
123 containing mutations to *clpA* and/or *clpP* (**Fig. 1**). ClpAP dependent degradation
124 of HapR is not unique to *V. cholerae*, but has previously been observed in *Vibrio*
125 *vulnificus* where ClpAP degrades the HapR homolog SmcR (12). In addition to
126 the ClpAP machine, it was shown that the Lon protease also plays a role in
127 SmcR degradation. So, we next sought to investigate the role of other protease
128 machines on induction of P_{chb} and HapR protein levels. Mutations to other Clp
129 components (the ClpS adaptor protein or the ClpX unfoldase*)* did not have a
130 marked impact on HapR protein levels. Also, a Δ*clpS* mutation did not affect P_{chb}
131 expression levels, while a Δ*clpX* mutation slightly decreased P_{chb} expression
132 (**Fig. 1**). Because HapR levels were not elevated in the Δ*clpX* mutant
133 background, however, the observed decrease in P_{chb} expression may be
134 attributed to a pleiotropic effect. In contrast to the effect of the Lon protease on
135 SmcR levels in *V. vulnificus*, we did not observe an impact of Δ*lonA* on HapR
136 levels in *V. cholerae*; and Δ*lonA*, correspondingly, did not affect P_{chb} expression
137 (**Fig. 1**). Together, these results establish that HapR is a repressor of P_{chb} and
138 that HapR levels are controlled specifically by the ClpAP protease in *V. cholerae*.

139
140 *HapR-mediated repression of P_{chb} occurs on chitinous surfaces*
141 Thus far, we have demonstrated that HapR is a repressor of P_{chb} that acts
142 downstream of ChiS activation using a Δ*cbp* mutation to induce ChiS activity.
143 Natural induction of this locus, however, occurs in the presence of chitin
144 oligosaccharides. So, we next wanted to test whether the repression of P_{chb} by
145 HapR was observed in a more physiologically relevant setting. To test this, we
146 cultured *V. cholerae* strains with CBP intact, a P_{chb}-mCherry reporter, and a
147 construct that constitutively expresses GFP (P_{const2}-GFP) on chitin beads (**Fig.**
148 **2A**). The P_{const2}-GFP construct [derived from the insulated proD promoter (13)]
149 served as an internal control for noise in gene expression and was used to
150 normalize P_{chb}-mCherry expression in single cells (see Methods for details).
151
152 When cells were cultured on chitin beads, both the parent strain and the Δ*hapR*
153 strain exhibited a bimodal distribution of P_{chb} expression (**Fig. 2A-D**). There were
154 at least two possible explanations for the observed bimodality in P_{chb} gene
155 expression in this experiment. One, the signaling pathway that leads to activation
156 of *chb* has switch-like behavior that results in a population that exhibits bimodality
157 in *chb* expression. Or two, the environment during growth on chitin beads is
158 heterogenous and only some cells within the population have access to the chitin
159 oligosaccharides necessary for activation of *chb*. Those cells that do not have
160 access to chitin do not activate P_{chb} expression (P_{chb} Off), while those that do
161 have access to chitin do induce P_{chb} expression (P_{chb} On). To differentiate
162 between these two possibilities, we genetically activated P_{chb} in the absence of
163 chitin by deleting *cbp*. If the signaling circuit responsible for P_{chb} activation has
164 switch like behavior, we would predict that bimodality in gene expression would
165 be maintained; however, if bimodality is the result of heterogenous access to
166 chitin oligosaccharides when cells are cultured on chitin beads, we would expect
167 bimodality to be lost. When P_{chb} is activated via a Δ*cbp* mutation, all cells in the
168 population are uniformly "P_{chb} On" (**Fig. 2E**) and the population becomes
169 unimodal (**Fig. 2F**). Thus, these results showed that only the "P_{chb} On" cells have
170 access to chitin oligosaccharides when grown on chitin beads. These results are
171 consistent with chitin-induction of natural competence genes on chitin beads,
172 where cells display bimodality in gene expression that is also likely due to
173 heterogeneous access to inducing chitin oligosaccharides (14).
174
175 Next, we tested whether HapR influenced activation of P_{chb} on chitin beads by
176 just assessing the expression level among "P_{chb} On" cells. As observed in bulk
177 populations, the Δ*hapR* strain exhibited a ~1.7 fold increase in P_{chb} expression
178 (**Fig. 2D**). This was also consistent with the ~2-fold increase in P_{chb} expression
179 observed in single cells when the population was induced via deletion of *cbp*
180 (**Fig. 2G**). Together, these results indicate that HapR is a *bona fide* repressor of
181 P_{chb} even under physiologically relevant inducing conditions.
182
183 *HapR repression of P_{chb} is conserved in other V. cholerae El Tor isolates*

184 Previously, it was suggested that HapR was actually an activator of P_{chb}
185 expression in the *V. cholerae* El Tor isolate A1552 (15). Specifically, the authors
186 showed that deletion of *hapR* resulted in a decrease in P_{chb} expression when
187 cells were cultured on chitin flakes. In the present study, we use the *V. cholerae*
188 El Tor isolate E7946 to study P_{chb} regulation. To assess if HapR exhibits different
189 effects on P_{chb} expression depending on the strain background, we assessed
190 expression of a P_{chb}-mCherry reporter in *hapR*$^+$ and Δ*hapR* derivatives of both
191 E7946 and A1552. Consistent with our previous results, we observed that P_{chb}
192 expression is elevated ~2-fold in the Δ*hapR* derivative of both strain
193 backgrounds, which is consistent with HapR acting as a repressor of this locus
194 (**Fig. S1**). It is unclear what explains the discrepancy between our findings and
195 those that were previously reported; however, these data suggest that they
196 cannot be attributed to differences between strain backgrounds.
197
198 *Deletion of HapR does not confer a growth advantage during growth on*
199 *chitobiose*
200 Our data indicate that in the absence of HapR, P_{chb} expression is elevated. The
201 *chb* locus encodes the genes required for uptake and degradation of the chitin
202 disaccharide, chitobiose. So next, we wanted to assess if the increased
203 expression of P_{chb} confers a fitness advantage to Δ*hapR* cells during growth on
204 chitobiose. To test this, we conducted competitive growth assays with a 1:1
205 mixture of a parent and a Δ*hapR* mutant strain on minimal medium with
206 chitobiose as the sole carbon source. We hypothesized that if the Δ*hapR* mutant
207 had a competitive growth advantage due to increased expression of *chb*, then it
208 should outcompete the parent strain in this assay. Even after ~48 generations of
209 growth on chitobiose, however, we did not observe a competitive advantage for
210 the Δ*hapR* mutant (**Fig. S2**). HapR is a global regulator that controls the
211 expression of dozens of genes. Thus, even though a Δ*hapR* mutant has
212 increased P_{chb} expression, there may be negative pleiotrophic effects associated
213 with the Δ*hapR* mutation that masks any competitive advantage of derepression
214 of P_{chb} in this mutant during growth on chitobiose.
215
216 *HapR binds P_{chb} in vitro and in vivo*
217 Thus far, our data suggest that HapR is a repressor of P_{chb}, but it does not
218 distinguish whether HapR is a direct or indirect regulator of this locus. To assess
219 if HapR could be regulating P_{chb} directly, we used an *in silico* approach to identify
220 putative HapR binding sites in P_{chb} based on consensus binding sequences
221 generated for the HapR homologs LuxR (from *Vibrio harveyi*) and SmcR (from *V.*
222 *vulnificus*) via chromatin immunoprecipitation sequencing (ChIP-seq) (16, 17).
223 Through this analysis, we identified two potential HapR binding sites in P_{chb} (**Fig.**
224 **3A**; exact sequences in **Fig. S3**). Interestingly, these binding sites (BSs) overlap
225 with other elements in the *chb* promoter required for transcriptional activation.
226 HapR BS 1 overlaps with the SlmA binding site, which is a critical activator of
227 P_{chb} expression (10). HapR BS 2 overlaps with the -35 signal, which is required
228 for RNA polymerase to bind to the promoter and initiate transcription. This

229 sequence analysis suggests that the repressive effect of HapR may be due to
230 HapR binding directly antagonizing SlmA and/or RNAP at this locus.
231
232 We next sought to determine whether HapR could directly bind to P_{chb} using both
233 *in vitro* and *in vivo* approaches. First, we tested whether HapR could bind to P_{chb}
234 *in vitro* using EMSA assays. Consistent with the presence of two HapR binding
235 sites in P_{chb}, we observed two shifts by EMSA when using a DNA probe of the
236 *chb* promoter (**Fig. 3B**). HapR does not regulate the ClpP promoter and thus did
237 not bind P_{clpP} (**Fig. 3B**), which is consistent with previous studies (18). EMSAs
238 were also done using 32 bp probes that encompassed each putative HapR BS
239 (probe sequences in **Fig. S3**). We observed that HapR was able to bind to both
240 probes, suggesting that HapR binds to both HapR BS 1 and HapR BS 2 (**Fig.**
241 **3C**). Next, we wanted to assess if HapR bound to P_{chb} *in vivo* via ChIP assays
242 under physiologically relevant conditions. To that end, we first generated a
243 FLAG-HapR strain that was functional for regulating P_{chb} expression (**Fig. S4**).
244 Using this strain in ChIP-qPCR assays, we found that P_{chb} was, indeed, bound by
245 HapR *in vivo*, while the negative control P_{clpP} locus was not bound by HapR (**Fig.**
246 **3D**). Together, these data demonstrate that HapR binds to P_{chb}, which suggests
247 that it may be a direct repressor of this locus.
248
249 *Quorum sensing regulates expression of P_{chb} through the cholera-specific*
250 *autoinducer CAI-1*
251 HapR is the master regulator of quorum sensing (QS) in *V. cholerae*, and is
252 highly expressed at high cell density (HCD). Thus far, we have only established
253 that HapR is a repressor of P_{chb} expression. Next, we wanted to probe the role of
254 QS in regulating P_{chb}. To that end, we sought to test the effect of mutations to
255 genes upstream of HapR in the *V. cholerae* QS cascade on P_{chb} induction and
256 HapR protein levels.
257
258 QS in *Vibrio* species is controlled by autoinducer-responsive sensor proteins that
259 indirectly modulate phosphorylation of the response regulator LuxO, which in turn
260 indirectly regulates production of HapR. When autoinducer concentrations are
261 low (*i.e.*, at low cell density (LCD)), multiple histidine kinase sensors acts as
262 kinases. This results in high levels of phosphorylated LuxO, which prevents
263 HapR production (**Fig. 4A**, left). By contrast, at high autoinducer concentrations
264 (*i.e.*, at HCD), the sensors act as phosphatases, which ultimately leads to
265 dephosphorylation of LuxO and allows for HapR production (**Fig. 4A**, right).
266
267 First, we assessed the impact of HCD on P_{chb} induction and HapR levels by
268 deleting *luxO*, which genetically locks cells in a HCD state. Induction of the
269 parent strain is tested under HCD conditions, thus, as expected, HapR levels
270 were similar between the parent and the Δ*luxO* mutant; accordingly, expression
271 of P_{chb} was also similar between the parent and Δ*luxO* (**Fig. 4B**). Next, we tested
272 the effect of LCD on P_{chb} and HapR expression by generating a $luxO^{D47E}$ mutant,
273 which mimics phosphorylated LuxO and genetically locks cells in a LCD state. In
274 this strain, we saw that P_{chb} expression increased and was correlated with a

275 decrease in HapR protein levels (**Fig. 4B**). Together, these data suggest that
276 HapR repression of P_{chb} is mediated through the canonical QS circuit.
277
278 Next, we wanted to move further upstream in the QS regulatory cascade to
279 address if distinct autoinducers differentially affected expression of P_{chb} and
280 HapR. There are potentially four histidine kinase sensors that coordinate QS-
281 dependent control of HapR expression (19); however, the autoinducer signal is
282 only known for two of these systems. The sensor LuxPQ is responsive to the
283 inter-species autoinducer AI-2, and the sensor CqsS is responsive to the *V.*
284 *cholerae*-specific autoinducer CAI-1 (**Fig. 4A**) (20). To assess the role of each
285 autoinducer in regulation of P_{chb}, we made mutations to the synthase genes
286 responsible for production of each autoinducer. LuxS makes AI-2 (21) and CqsA
287 makes CAI-1 (20) (**Fig. 4A**). In a strain that no longer produces AI-2 (Δ*luxS*),
288 expression of P_{chb} was similar to that observed in the parent and HapR levels
289 remained similar in these two strains (**Fig. 4B**). By contrast, a strain that is
290 unable to produce CAI-1 (Δ*cqsA*) had increased expression of P_{chb}, likely due to
291 the low level of HapR produced (**Fig. 4B**). The observed decrease in P_{chb}
292 expression in the Δ*cqsA* background was, indeed, due to a lack of CAI-1
293 production as exogenously adding back synthetic CAI-1 restored HapR levels
294 and repression of P_{chb} to the parent level (**Fig. 4B**). In addition, a strain that does
295 not make CAI-1 induced P_{chb} to the same level as a strain that does not produce
296 CAI-1 or HapR (**Fig. 4B**). This epistasis indicates that CAI-1 production and
297 HapR are involved in the same regulatory pathway for modulating expression of
298 P_{chb}. These data support previous results, which indicate that CqsS signaling
299 plays a dominant role in regulating HapR (14, 20, 22, 23). Together, these results
300 indicate that P_{chb} expression is strongly influenced by QS signaling mediated by
301 the *V. cholerae*-specific autoinducer CAI-1 and less via the inter-species
302 autoinducer AI-2.
303
304 **Discussion**
305 Here, we show that HapR acts as a repressor of chitobiose utilization genes in *V.*
306 *cholerae*. When this organism forms communities on a chitinous surface, chitin
307 induces expression of P_{chb} through activation of the chitin sensor ChiS (**Fig. 5**).
308 *V. cholerae* then modulates P_{chb} expression depending on the presence of other
309 *V. cholerae* cells, which it senses via the *V. cholerae*-specific autoinducer CAI-1.
310 At low CAI-1 concentrations, P_{chb} expression is high because the repressor HapR
311 is produced at a low level (**Fig. 5A**). At high CAI-1 concentrations, HapR is
312 produced at higher levels and can repress P_{chb} expression (**Fig. 5B**). Because
313 HapR directly binds to P_{chb} both *in vitro* and *in vivo*, we speculate that this
314 repressive effect is direct.
315
316 When HapR is produced, it gets proteolyzed by the ClpAP machine (**Fig. 5B**).
317 While the dynamic range of HapR-dependent P_{chb} repression is only ~2-fold
318 when ClpAP is intact, the dynamic range of repression increases to ~7-fold in the
319 absence of ClpAP. Thus, it is tempting to speculate that regulation of ClpAP may
320 modulate P_{chb} expression under some conditions. Currently, however, little is

321 known about the regulation of ClpAP in *V. cholerae*. ClpAP is induced during
322 heat shock in *V. vulnificus* (12). Also, in *E. coli*, ClpP expression is induced
323 during heat shock (24-26). Thus, it is believed that the ClpP protease plays a role
324 in the heat shock response. In *Bacillus subtilis*, ClpP is upregulated under
325 various stress conditions, suggesting that this protease may also be induced by a
326 general stress response (27). Thus, one possibility is that stress-dependent
327 regulation of ClpAP indirectly regulates P_{chb}. It has also been hypothesized that
328 *V. cholerae* makes use of proteolysis machines to rapidly respond to changes in
329 their environment; namely, the transition from the human gut to the aquatic
330 environment after infection (28). ClpAP acting as an activator of P_{chb} may be a
331 way for cells to rapidly induce expression of a locus that is not important in the
332 human gut, but is useful for survival in its aquatic reservoir. Consistent with this
333 idea, *chb* is induced late in infection, suggesting this is a critical locus for
334 preparing to re-enter the aquatic environment after infection of a host (29).
335
336 The mechanisms underlying distinct responses to AI-2 or CAI-1 remain a topic of
337 interest in QS. It has been shown that the CAI-1 sensor CqsS plays a dominant
338 role over LuxPQ in modulating HapR levels. Thus, it remains possible that the
339 presence of CAI-1 allows for more robust regulation of HapR-regulated genes.
340 Indeed, CAI-1 has been shown to be critical for expression of the virulence factor
341 *hapA* (23), natural transformation (30), and for repressing chitobiose utilization as
342 shown in this study. HapA has been implicated in mediating *V. cholerae*
343 detachment from host epithelial cells, thereby promoting dissemination of cells
344 back into the aquatic environment (31, 32); natural transformation and chitin
345 utilization aid in *V. cholerae* fitness in the marine environment. By contrast,
346 expression of the major subunit of the toxin co-regulated pilus *tcpA* was shown to
347 be primarily regulated by AI-2 (22). It is tempting to speculate that CAI-1 controls
348 *V. cholerae* behaviors important for marine survival, whereas AI-2 controls
349 behaviors involved in infection (where the community is complex and has many
350 bacteria producing AI-2). It has been hypothesized that sensing both of these
351 autoinducers plays a critical role in biofilm dispersal, and that only when both are
352 sensed, *V. cholerae* cells are induced to leave a surface (i.e. QS works as a
353 coincidence detector for both signals) (22). Thus, signaling via distinct
354 autoinducers may allow *V. cholerae* to modulate responses depending on the
355 context of the environment they are inhabiting.
356
357 The data we present here suggests that at HCD, *V. cholerae* dampens its
358 expression of a chitin utilization locus. Below, we speculate on a few reasons
359 why this regulation may be advantageous. *V. cholerae* must secrete chitinases
360 that enzymatically degrade long chain insoluble chitin polymers into soluble chitin
361 oligosacchardies that can then be taken up and catabolized. This is an
362 energetically costly process, and as a result, liberated chitin is a valuable “public
363 good” in the context of a chitin biofilm (33). Thus, one possible explanation is that
364 QS regulation of chitin utilization allows *V. cholerae* to modulate chitin uptake
365 based on the composition of its microbial community. When other *V. cholerae*
366 cells are nearby, which will signal via the *V. cholerae*-specific autoinducer CAI-1,

367 chitin uptake may decrease among individual cells within the population in an
368 effort to “share” liberated chitin. By contrast, sensing the inter-species AI-2 does
369 not suppress chitin uptake and utilization.
370
371 Another possibility is that this regulation allows *V. cholerae* to control its
372 production of toxic metabolites. In a previous study, it was shown that cells in a
373 HCD state alter their metabolic flux to produce neutral byproducts as opposed to
374 organic acids (34). This regulation allows for a more stable community; by
375 contrast, cells locked in a LCD state will excrete harmful metabolic byproducts,
376 which leads to the demise of the community. Thus, it is possible that repressing
377 chitin uptake and utilization also helps slow the rate of metabolism to prevent the
378 accumulation of toxic intermediates in a dense community setting.
379
380 **Materials & Methods**
381 *Bacterial strains and culture conditions*
382 *V. cholerae* strains were routinely grown in LB medium and on LB agar
383 supplemented when necessary with Carbenicillin (20 µg/mL or 50 µg/mL),
384 Kanamycin (50 µg/mL), Spectinomycin (200 µg/mL), Trimethoprim (10 µg/mL),
385 and/or Chloramphenicol (2 µg/mL).
386
387 *Transposon mutagenesis*
388 Transposon mutant libraries were generated with a $Carb^R$ mini-Tn10 transposon
389 exactly as previously described (35). Briefly, the transposon mutagenesis
390 plasmid pDL1086 was first mated into P_{chb}-*lacZ* Δ*cbp* or P_{chb}-*lacZ* Δ*clpA* Δ*cbp*
391 parent strains. The parent strains also carried a P_{chb}-mCherry reporter at an
392 ectopic site to ensure that candidate transposon mutants affected expression of
393 P_{chb} and did not simply disrupt the P_{chb}-*lacZ* reporter. The activator screen parent
394 carried an additional copy of ChiS, as this is a known activator of this locus.
395 Transposition was induced by plating cultures on LB agar supplemented with 50
396 µg/mL Carb at 42°C. To screen colonies, plates also contained 40 µg/mL X-gal
397 and 5 mM IPTG. IPTG was added to competitively inhibit the basal activity of the
398 P_{chb}-*lacZ* reporter.
399
400 *Generating mutant strains*
401 *V. cholerae* E7946 served as the parent for all strains generated in this study,
402 except for those used in **Fig. S1** where we compare E7946 to A1552 (36, 37).
403 Mutant constructs were generated using splicing-by-overlap extension PCR
404 exactly as previously described (38). Transformations and cotransformations
405 were carried out by chitin-induced natural transformation exactly as previously
406 described (39, 40). Mutant strains were confirmed by PCR and/or sequencing. A
407 complete list of strains and primers used in this study are outlined in **Table S1**
408 and **Table S2**, respectively.
409
410 *Measuring GFP and mCherry fluorescence in bulk populations*
411 GFP and mCherry fluorescence in reporter strains was determined exactly as
412 previously described (41). Briefly, single colonies were grown in LB

413 (supplemented with 10 μM CAI-1 where noted) overnight at 30°C. The next day,
414 cells were washed and resuspended to an OD of 1.0 in instant ocean medium
415 (7g/L; Aquarium systems). Fluorescence was determined on a BioTek H1M plate
416 reader. For GFP measurements, excitation was set to 500 nm and emission was
417 set to 540 nm; for mCherry measurements, excitation was set to 580 nm and
418 emission was set to 610 nm.
419
420 *Antibody generation*
421 Purified LuxR protein (300 μg; purified as previously described (42)) was sent to
422 Cocalico Biologicals Inc. for serial injection into a rabbit host for antibody
423 generation. Serum obtained from the third bleed has been used for Western
424 analyses.
425
426 *Western blotting*
427 From overnight cultures, cells were concentrated to an OD_{600} of 20 in instant
428 ocean medium. Cells were lysed on a FastPrep-24 Classic Instrument at 4°C,
429 then lysates were clarified by centrifugation. Lysates were then boiled with an
430 equal volume of 2x SDS PAGE sample buffer (220 mM Tris pH 6.8, 25%
431 glycerol, 1.2% SDS, 0.02% Bromophenol Blue, and 5% β-mercaptoethanol).
432 Proteins were separated by SDS polyacrylamide gel electrophoresis,
433 electropheretically transferred to a PVDF membrane, and probed with rabbit
434 polyconal α-LuxR serum or mouse monoclonal α-RpoA (Biolegend) primary
435 antibodies. LuxR is the HapR homolog in *Vibrio harveyi* and has 72% identity and
436 86% similarity to *V. cholerae* HapR. Blots were then incubated with α-rabbit or α-
437 mouse HRP conjugated secondary antibodies, developed using Pierce ECL
438 Western Blotting Substrate (ThermoFisher), and exposed to film.
439
440 *Chitin bead culturing*
441 Chitin beads (200 μL of a 50% slurry; NEB) and overnight cultures of the
442 indicated strains were washed with defined artificial salt water medium (DASW),
443 which was prepared exactly as previously described (5). Chitin beads were
444 inoculated with *V. cholerae* cells to an OD of 0.1 in a final volume of 5 mL in a
445 Costar 6-well plate (Corning). Chitin mixtures were incubated statically at 30°C
446 for 7 days before imaging.
447
448 *Microscopy data collection and analysis*
449 To image chitin beads, cultured beads were gently transferred to a coverslip
450 using wide-bore pipette tips. To image chitin grown cells, chitin bead reactions
451 were vortexed then centrifuged at 250 x g for 1 minute. Cells found in the
452 supernatant were transferred to a coverslip. To image Δ*cbp* strains, overnight
453 cultures grown in LB were resuspended to an OD_{600} of 0.2 in DASW and then
454 transferred to a coverslip. Samples on the coverslip were placed under a 0.2%
455 gelzan pad and imaged on an inverted Nikon Ti-2 microscope with a Plan Apo
456 60x objective, YFP & mCherry filter cubes, a Hamamatsu ORCAFlash 4.0
457 camera, and Nikon NIS Elements imaging software.
458

459 The strains used to examine P_{chb} expression across a population contained 1) a
460 P_{chb}-mCherry reporter and 2) a reporter that drove constitutive expression of
461 GFP, P_{const2}-GFP. By using these reporters, the expression of the P_{chb}-mCherry
462 could be normalized to GFP expression in each cell. Images were analyzed on
463 Fiji using the MicrobeJ plugin (43) to determine mean intensity of cells in the YFP
464 and mCherry channels. GFP was assessed using the YFP channel to avoid
465 background fluorescence from chitin beads, which was stronger in the GFP
466 channel. Background fluorescence was subtracted from each channel and the
467 mCherry / GFP fluorescence was determined for each individual cell.
468
469 *HapR protein purification*
470 A plasmid expressing a hexahistidine-tagged *hapR* wild-type allele was
471 generated using Gibson assembly. The hapR insert was amplified from *V.*
472 *cholerae* E7946 and inserted into a pET28b vector (Novagen) using the primers
473 listed in **Table S2**. The plasmid was then electroporated into *E. coli* BL21(DE3)
474 for protein overexpression. This strain was grown overnight in LB medium with
475 kanamycin, back-diluted 1:100 into 1 L of LB medium with kanamycin, and grown
476 to an OD_{600} of 0.4-0.6 at 30°C. Expression of HapR was induced by IPTG to a
477 final concentration of 1 mM and cultures grown for 4 h shaking at 30°C. The cells
478 were pelleted and frozen at -80°C. The pellet was resuspended in 25 mL buffer A
479 (25 mM Tris pH 8, 500 mM NaCl), and an Avestin EmulfiFlex-C3 emulsifier was
480 used to lyse cells. The soluble lysate was applied to a HisTrap HP Ni-NTA
481 column using an Äkta Pure FPLC in buffer A and eluted from the column with a
482 gradient of buffer B (25 mM Tris pH 8, 500 mM NaCl, 1 M imidazole). The
483 purified protein was concentrated to approximately 5 ml using Sartorius Vivaspin
484 Turbo 10,000 MWCO centrifugal concentrators. The sample was manually
485 injected into the Äkta Pure and separated via size exclusion chromatography on
486 a HiLoad™ 16/600 Superdex™ 75 pg column equilibrated with gel filtration buffer
487 (25 mM Tris pH 7.5, 200 mM NaCl). Eluted fractions were analyzed by SDS-
488 PAGE, pooled, and concentrated using the same centrifugal concentrators
489 previously mentioned. The samples were then immediately frozen in liquid
490 nitrogen with a final concentration of 10% glycerol and stored at -80°C.
491
492 *Electrophoretic mobility shift assay (EMSA)*
493 Binding reactions contained 10 mM tris HCl pH 7.5, 1 mM EDTA, 10 mM KCl, 1
494 mM DTT, 50 µg/mL BSA, 0.1 mg/mL salmon sperm DNA, 5% glycerol, 1 nM of a
495 Cy5 labeled DNA probe, and HapR at the indicated concentrations (diluted in 10
496 mM tris pH 7.5, 10 mM KCl, 1 mM DTT, and 5% glycerol). Reactions were
497 incubated at room temperature for 20 minutes in the dark, then
498 electrophoretically separated on polyacrylamide gels in 0.5x Tris Borate EDTA
499 (TBE) buffer. Gels were imaged for Cy5 fluorescence on a Typhoon-9210
500 instrument. Short DNA probes (30bp) were made by end-labeling one primer of a
501 complementary pair (primers listed in **Table S2**) using 20 µM Cy5-dCTP and
502 Terminal deoxynucleotidyl Transferase (TdT; Promega). Complementary primers
503 (one labeled with Cy5 and the other unlabeled) were annealed by slow cooling at
504 equimolar concentrations in annealing buffer (10 mM Tris pH 7.5 and 50 mM

505 NaCl). P_{chb} and P_{clpP} probes were made by Phusion PCR, where Cy5-dCTP was
506 included in the reaction at a level that would result in incorporation of 1–2 Cy5
507 labeled nucleotides in the final probe as previously described.
508
509 *ChIP-qPCR assays*
510 Assays were carried out exactly as previously described (7). Briefly, overnight
511 cultures were diluted to an OD_{600} of 0.08 and then grown for 6 hours at 30°C.
512 Cultures were crosslinked using 1% paraformaldehyde, then quenched with a 1.2
513 molar excess of Tris. Cells were washed with PBS and stored at -80°C overnight.
514 The next day, cells were resuspended in lysis buffer (1x FastBreak cell lysis
515 reagent (Promega), 50 µg/mL lysozyme, 1% Triton X-100, 1 mM PMSF, and 1x
516 protease inhibitor cocktail; 100x inhibitor cocktail contained the following: 0.07
517 mg/mL phosphoramidon (Santa Cruz), 0.006 mg/mL bestatin
518 (MPbiomedicals/Fisher Scientific), 1.67 mg/mL AEBSF (DOT Scientific), 0.07
519 mg/mL pepstatin A (Gold Bio), 0.07 mg/mL E64 (Gold Bio)) and then lysed by
520 sonication, resulting in a DNA shear size of ~500 bp. Lysates were incubated
521 with Anti-FLAG M2 Magnetic Beads (Sigma), washed to remove unbound
522 proteins, and then bound protein-DNA complexes were eluted off with SDS.
523 Samples were digested with Proteinase K, then crosslinks were reversed. DNA
524 samples were cleaned up and used as template for quantitative PCR (qPCR)
525 using iTaq Universal SYBR Green Supermix (Bio-Rad) and primers specific for
526 the genes indicated (primers are listed in **Table S2**) on a Step-One qPCR
527 system. Standard curves of genomic DNA were included in each experiment and
528 were used to determine the abundance of each amplicon in the input (derived
529 from the lysate prior to ChIP) and output (derived from the samples after ChIP).
530 Primers to amplify *rpoB* served as a baseline control in this assay because HapR
531 does not bind this locus. Data are reported as 'Fold Enrichment', which is defined
532 as the ratio of the test promoter (P_{chb} or P_{clpP}) / *rpoB* found in the output divided
533 by the same ratio found in the input.
534
535 *Chitobiose competition*
536 Overnight cultures grown in LB were washed with M9 medium and mixed 1:1.
537 For each growth reaction, 10^2 cells of this mixture was added to M9 medium
538 supplemented with 0.2% chitobiose and 10 µM synthetic CAI-1 and grown
539 shaking at 30°C for 24 hours. After 24 hours, ~10^2 cells from this mixture was
540 used to inoculate fresh growth reactions to achieve additional generations of
541 growth on chitobiose. This was repeated a third time after another 24 hours. CAI-
542 1 was supplemented throughout these experiments to ensure consistently high
543 levels of HapR expression throughout transfer steps. After each 24 hour growth
544 period, the CFU/mL was determined for each strain in the mixture by dilution
545 plating on LB agar supplemented with X-gal. Competing strains were discerned
546 by blue/white screening as one strain was *lacZ*$^+$ and the other was Δ*lacZ*. *V.*
547 *cholerae* can grow on chitobiose through the activity of two sugar transporters:
548 the GlcNAc PTS transporter (VC0995) or the chitobiose ABC transporter
549 (VC0616-0620). Because we wanted to study the regulation of the transporter
550 encoded within the *chb* locus, strains for this assay had a deletion in VC0995,

which renders growth on chitobiose dependent on the *chb* locus as previously described (10).

Statistics

Statistical comparisons were determined using Student's t-test or One-way ANOVA with Tukey's post-test using GraphPad Prism software.

Acknowledgements

We thank Ryan Chaparian for offering experimental advice, David Grainger for helpful discussions, and Wai-Leung Ng for providing synthetic CAI-1. This work was supported by grant R35GM128674 from the National Institutes of Health to ABD and R35GM124698 from the National Institutes of Health to JVK.

565 **References**
566

567 1. Pruzzo C, Vezzulli L, & Colwell RR (2008) Global impact of Vibrio
568 cholerae interactions with chitin. *Environ Microbiol* 10(6):1400-1410.
569 2. Colwell RR*, et al.* (2003) Reduction of cholera in Bangladeshi villages by
570 simple filtration. *Proc Natl Acad Sci U S A* 100(3):1051-1055.
571 3. Huq A*, et al.* (2010) Simple sari cloth filtration of water is sustainable and
572 continues to protect villagers from cholera in Matlab, Bangladesh. *mBio*
573 1(1).
574 4. Meibom KL*, et al.* (2004) The Vibrio cholerae chitin utilization program.
575 *Proc Natl Acad Sci U S A* 101(8):2524-2529.
576 5. Meibom KL, Blokesch M, Dolganov NA, Wu CY, & Schoolnik GK (2005)
577 Chitin induces natural competence in Vibrio cholerae. *Science*
578 310(5755):1824-1827.
579 6. Li X & Roseman S (2004) The chitinolytic cascade in Vibrios is regulated
580 by chitin oligosaccharides and a two-component chitin catabolic
581 sensor/kinase. *Proc Natl Acad Sci U S A* 101(2):627-631.
582 7. Klancher CAY, S.; Dalia, T. N.; Dalia, A. B. (2020) ChiS is a noncanonical
583 DNA-binding hybrid sensor kinase that directly regulates the chitin
584 utilization program in Vibrio cholerae. *In review*.
585 8. Yamamoto S & Ohnishi M (2017) Glucose-Specific Enzyme IIA of the
586 Phosphoenolpyruvate:Carbohydrate Phosphotransferase System
587 Modulates Chitin Signaling Pathways in Vibrio cholerae. *J Bacteriol*
588 199(18).
589 9. Blokesch M (2012) Chitin colonization, chitin degradation and chitin-
590 induced natural competence of Vibrio cholerae are subject to catabolite
591 repression. *Environ Microbiol* 14(8):1898-1912.
592 10. Klancher CA, Hayes CA, & Dalia AB (2017) The nucleoid occlusion
593 protein SlmA is a direct transcriptional activator of chitobiose utilization in
594 Vibrio cholerae. *PLoS Genet* 13(7):e1006877.
595 11. Sauer RT & Baker TA (2011) AAA+ proteases: ATP-fueled machines of
596 protein destruction. *Annu Rev Biochem* 80:587-612.
597 12. Lee KJ, Jung YC, Park SJ, & Lee KH (2018) Role of Heat Shock
598 Proteases in Quorum-Sensing-Mediated Regulation of Biofilm Formation
599 by Vibrio Species. *mBio* 9(1).
600 13. Davis JH, Rubin AJ, & Sauer RT (2011) Design, construction and
601 characterization of a set of insulated bacterial promoters. *Nucleic Acids*
602 *Res* 39(3):1131-1141.
603 14. Lo Scrudato M & Blokesch M (2012) The regulatory network of natural
604 competence and transformation of Vibrio cholerae. *PLoS Genet*
605 8(6):e1002778.
606 15. Sun S, Tay QX, Kjelleberg S, Rice SA, & McDougald D (2015) Quorum
607 sensing-regulated chitin metabolism provides grazing resistance to Vibrio
608 cholerae biofilms. *ISME J* 9(8):1812-1820.
609 16. van Kessel JC, Ulrich LE, Zhulin IB, & Bassler BL (2013) Analysis of
610 activator and repressor functions reveals the requirements for

611 transcriptional control by LuxR, the master regulator of quorum sensing in
612 Vibrio harveyi. *mBio* 4(4).
613 17. Lee DH*, et al.* (2008) A consensus sequence for binding of SmcR, a Vibrio
614 vulnificus LuxR homologue, and genome-wide identification of the SmcR
615 regulon. *J Biol Chem* 283(35):23610-23618.
616 18. Chaparian RR, Tran MLN, Miller Conrad LC, Rusch DB, & van Kessel JC
617 (2020) Global H-NS counter-silencing by LuxR activates quorum sensing
618 gene expression. *Nucleic Acids Res* 48(1):171-183.
619 19. Jung SA, Chapman CA, & Ng WL (2015) Quadruple quorum-sensing
620 inputs control Vibrio cholerae virulence and maintain system robustness.
621 *PLoS Pathog* 11(4):e1004837.
622 20. Miller MB, Skorupski K, Lenz DH, Taylor RK, & Bassler BL (2002) Parallel
623 quorum sensing systems converge to regulate virulence in Vibrio
624 cholerae. *Cell* 110(3):303-314.
625 21. Surette MG, Miller MB, & Bassler BL (1999) Quorum sensing in
626 Escherichia coli, Salmonella typhimurium, and Vibrio harveyi: a new family
627 of genes responsible for autoinducer production. *Proc Natl Acad Sci U S A*
628 96(4):1639-1644.
629 22. Bridges AA & Bassler BL (2019) The intragenus and interspecies quorum-
630 sensing autoinducers exert distinct control over Vibrio cholerae biofilm
631 formation and dispersal. *PLoS Biol* 17(11):e3000429.
632 23. Hurley A & Bassler BL (2017) Asymmetric regulation of quorum-sensing
633 receptors drives autoinducer-specific gene expression programs in Vibrio
634 cholerae. *PLoS Genet* 13(5):e1006826.
635 24. Kroh HE & Simon LD (1990) The ClpP component of Clp protease is the
636 sigma 32-dependent heat shock protein F21.5. *J Bacteriol* 172(10):6026-
637 6034.
638 25. Grossman AD, Erickson JW, & Gross CA (1984) The htpR gene product
639 of E. coli is a sigma factor for heat-shock promoters. *Cell* 38(2):383-390.
640 26. Katayama Y*, et al.* (1988) The two-component, ATP-dependent Clp
641 protease of Escherichia coli. Purification, cloning, and mutational analysis
642 of the ATP-binding component. *J Biol Chem* 263(29):15226-15236.
643 27. Gerth U, Kruger E, Derre I, Msadek T, & Hecker M (1998) Stress induction
644 of the Bacillus subtilis clpP gene encoding a homologue of the proteolytic
645 component of the Clp protease and the involvement of ClpP and ClpX in
646 stress tolerance. *Molecular microbiology* 28(4):787-802.
647 28. Pennetzdorfer N*, et al.* (2019) Regulated Proteolysis in Vibrio cholerae
648 Allowing Rapid Adaptation to Stress Conditions. *Front Cell Infect Microbiol*
649 9:214.
650 29. Schild S*, et al.* (2007) Genes induced late in infection increase fitness of
651 Vibrio cholerae after release into the environment. *Cell Host Microbe*
652 2(4):264-277.
653 30. Suckow G, Seitz P, & Blokesch M (2011) Quorum sensing contributes to
654 natural transformation of Vibrio cholerae in a species-specific manner. *J*
655 *Bacteriol* 193(18):4914-4924.

31. Benitez JA*, et al.* (1997) Adherence of Vibrio cholerae to cultured differentiated human intestinal cells: an in vitro colonization model. *Infect Immun* 65(8):3474-3477.
32. Benitez JA, Silva AJ, & Finkelstein RA (2001) Environmental signals controlling production of hemagglutinin/protease in Vibrio cholerae. *Infect Immun* 69(10):6549-6553.
33. Drescher K, Nadell CD, Stone HA, Wingreen NS, & Bassler BL (2014) Solutions to the public goods dilemma in bacterial biofilms. *Curr Biol* 24(1):50-55.
34. Hawver LA, Giulietti JM, Baleja JD, & Ng WL (2016) Quorum Sensing Coordinates Cooperative Expression of Pyruvate Metabolism Genes To Maintain a Sustainable Environment for Population Stability. *mBio* 7(6).
35. McDonough E, Kamp H, & Camilli A (2016) Vibrio cholerae phosphatases required for the utilization of nucleotides and extracellular DNA as phosphate sources. *Molecular microbiology* 99(3):453-469.
36. Miller VL, DiRita VJ, & Mekalanos JJ (1989) Identification of toxS, a regulatory gene whose product enhances toxR-mediated activation of the cholera toxin promoter. *J Bacteriol* 171(3):1288-1293.
37. Yildiz FH, Liu XS, Heydorn A, & Schoolnik GK (2004) Molecular analysis of rugosity in a Vibrio cholerae O1 El Tor phase variant. *Molecular microbiology* 53(2):497-515.
38. Dalia AB, Lazinski DW, & Camilli A (2013) Characterization of undermethylated sites in Vibrio cholerae. *J Bacteriol* 195(10):2389-2399.
39. Dalia AB, McDonough E, & Camilli A (2014) Multiplex genome editing by natural transformation. *Proc Natl Acad Sci U S A* 111(24):8937-8942.
40. Dalia AB (2018) Natural Cotransformation and Multiplex Genome Editing by Natural Transformation (MuGENT) of Vibrio cholerae. *Methods Mol Biol* 1839:53-64.
41. Dalia AB (2016) RpoS is required for natural transformation of Vibrio cholerae through regulation of chitinases. *Environ Microbiol* 18(11):3758-3767.
42. Chaparian RR, Olney SG, Hustmyer CM, Rowe-Magnus DA, & van Kessel JC (2016) Integration host factor and LuxR synergistically bind DNA to coactivate quorum-sensing genes in Vibrio harveyi. *Molecular microbiology* 101(5):823-840.
43. Ducret A, Quardokus EM, & Brun YV (2016) MicrobeJ, a tool for high throughput bacterial cell detection and quantitative analysis. *Nat Microbiol* 1(7):16077.

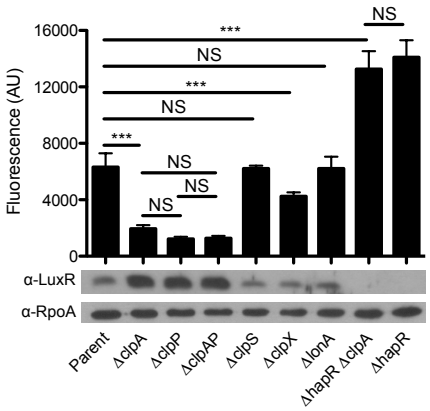

Figure 1. *HapR is a repressor of P_{chb} that is degraded by the ClpAP protease.* Expression of a P_{chb}-GFP reporter and HapR protein levels were determined in the indicated mutant strains. The parent strain contained a P_{chb}-GFP reporter and a Δ*cbp* mutation. A representative western blot is shown below bars to indicate the protein levels for HapR and RpoA (a loading control) in the corresponding strains. Fluorescence of cultures was determined on a plate reader from at least six independent biological replicates and is shown as the mean ± SD. Statistical comparisons were made by one-way ANOVA with Tukey's post-test. NS, not significant. ***, $p < 0.001$.

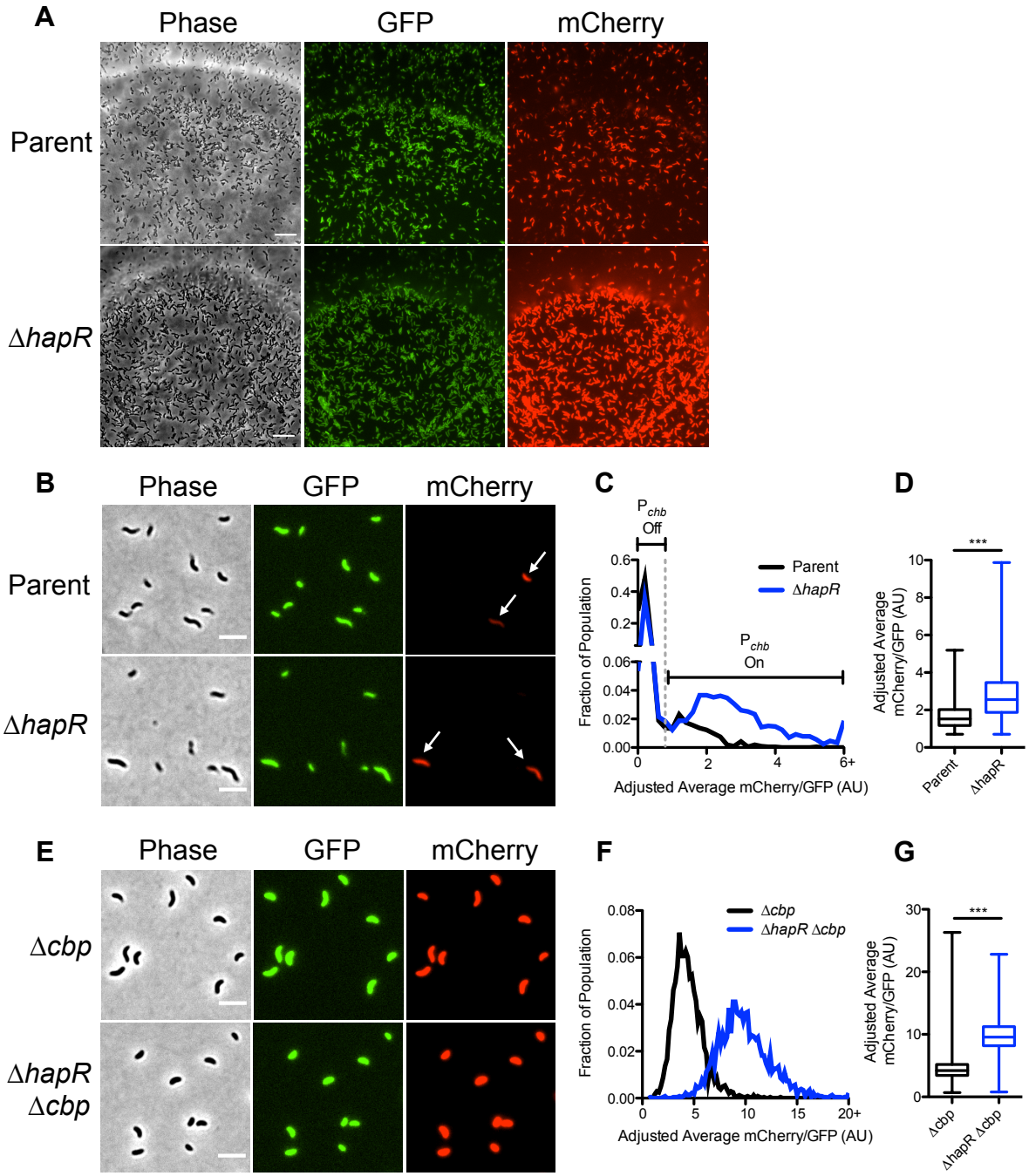

Figure 2. *HapR-mediated repression of P_{chb} occurs on chitinous surfaces.* **A**) Representative images of the indicated *V. cholerae* strains grown on chitin beads. The parent strain background contains both a P_{chb}-mCherry reporter and a P_{const2}-GFP construct, which exhibits constitutive GFP expression. Scale bar = 10 µm. **B-D**) P_{chb} expression in the indicated *V. cholerae cbp*$^+$ strains grown on chitin beads. **B**) Representative images of cells that were vortexed off chitin beads. Arrows demarcate cells where P_{chb} expression is induced ("P_{chb} On" cells). Scale bar = 4 µm. **C**) Histogram showing the relative expression of the P_{chb}-mCherry reporter. n = 2120 for Parent; n = 2191 for Δ*hapR.* Data shown are from two independent biological replicates. **D**) Box and whisker plot showing

733 average mCherry intensity of the "P_{chb} On" populations shown in **C**. Box
734 represents the first quartile, median, and third quartile while whiskers represent
735 the minimum and maximum values; n = 293 for Parent; n = 1092 for Δ*hapR.* **E-G**)
736 P_{chb} expression of the indicated *V. cholerae* strains where P_{chb} expression is
737 induced via deletion of *cbp*. **E**) Representative images of cells grown in the
738 absence of chitin. Scale bar = 4 µm. **F**) Histogram showing the relative
739 expression of a P_{chb}-mCherry reporter in the indicated *V. cholerae* strains. n =
740 2407 for Δ*cbp*; n = 2313 for Δ*hapR* Δ*cbp.* Data shown are from two independent
741 biological replicates. **G**) Box and whisker plot showing average mCherry intensity
742 of the populations depicted in **F**. Box represents the first quartile, median, and
743 third quartile while whiskers represent the minimum and maximum values; n =
744 2407 for WT; n = 2313 for Δ*hapR.* Statistical comparisons in **D** and **G** were made
745 using Student's t-test. ***, $p < 0.001$.
746

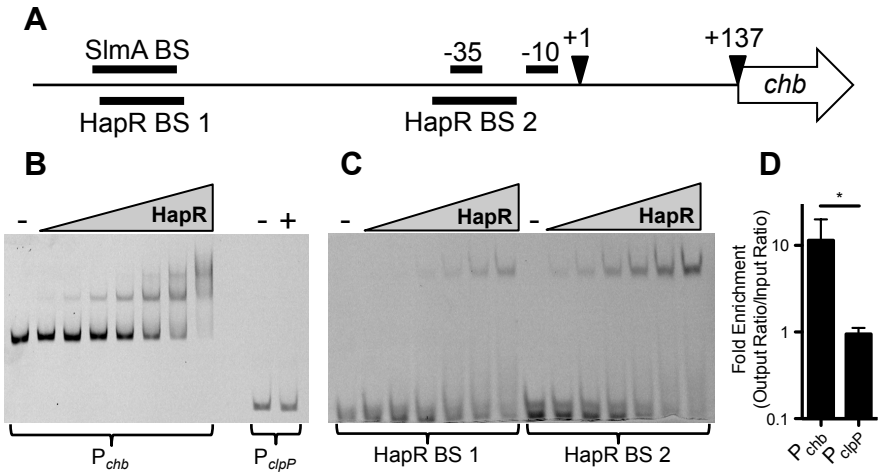

Figure 3. *HapR binds P_{chb} in vitro and in vivo.* **A**) Promoter map of P_{chb} highlighting putative HapR binding sites. Other sites required for P_{chb} activation (the SlmA binding site and the -35 and -10 signals) are highlighted. Also shown is the transcriptional start site (+1) and the translational start site (+137). **B**) A representative EMSA using HapR and Cy5-labeled DNA probes of the indicated promoters. The P_{chb} probe was incubated with (from left to right) 0 nM (-), 12.5 nM, 25 nM, 50 nM, 100 nM, 200 nM, 400 nM, or 800 nM purified HapR. The P_{clpP} probe was incubated with 0 nM (-) or 800 nM HapR (+). **C**) A representative EMSA using HapR and 32 bp Cy5-labeled probes encompassing each of the putative HapR binding sites within the *chb* promoter. The 32 bp probes were incubated with (from left to right) 0 nM (-), 100 nM, 200 nM, 400 nM, 800 nM, 1.6 μM, or 3.2 μM purified HapR. **D**) ChIP-qPCR assays showing enrichment of the indicated promoters relative to *rpoB*, a reference locus that HapR does not bind to. Data are from five independent biological replicates and shown as the mean ± SD. Statistical comparisons were made by Student's t-test. *, p = 0.0240.

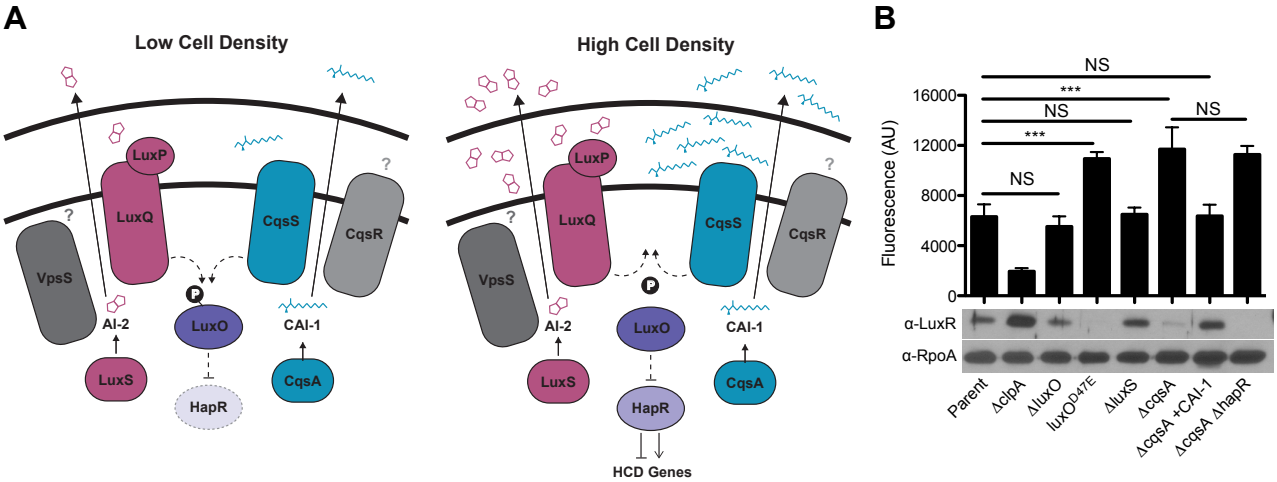

764
765 **Figure 4.** *Quorum sensing regulates expression of P_{chb} through the cholera-*
766 *specific autoinducer CAI-1*. **A**) Model of QS regulation in *V. cholerae*. There are
767 four sensor kinases that contribute to canonical QS in *V. cholerae* to regulate
768 HapR production: LuxQ, CqsS, VpsS, and CqsR. The signals for VpsS and CqsR
769 are unknown. LuxPQ senses the interspecies autoinducer AI-2 and CqsS senses
770 the *V. cholerae*-specific autoinducer CAI-1. AI-2 is produced by the LuxS
771 synthase and CAI-1 is produced by the CqsA synthase. (Left) At low cell density,
772 the LuxQ and CqsS sensors act as kinases, resulting in phosphorylation of LuxO,
773 which subsequently decreases expression of HapR. (Right) At high cell density
774 when concentrations of AI-2 and CAI-1 are high, LuxQ and CqsS act as
775 phosphatases, which results in dephosphorylation of LuxO, and subsequent
776 activation of HapR expression. **B**) Expression of a P_{chb}-GFP reporter and HapR
777 protein levels were determined in the indicated strains. The parent strain contains
778 a P_{chb}-GFP reporter and a Δ*cbp* mutation. A representative western blot is shown
779 below the bars to indicate the protein levels for HapR and RpoA (a loading
780 control) in the corresponding strains. Statistical comparisons were made by one-
781 way ANOVA with Tukey's post-test. NS, not significant. ***, $p < 0.001$. The P_{chb}-
782 GFP fluorescence data for "Parent" and "ΔclpA" are identical to the data
783 presented in **Fig. 1** and were included here to ease comparisons.
784

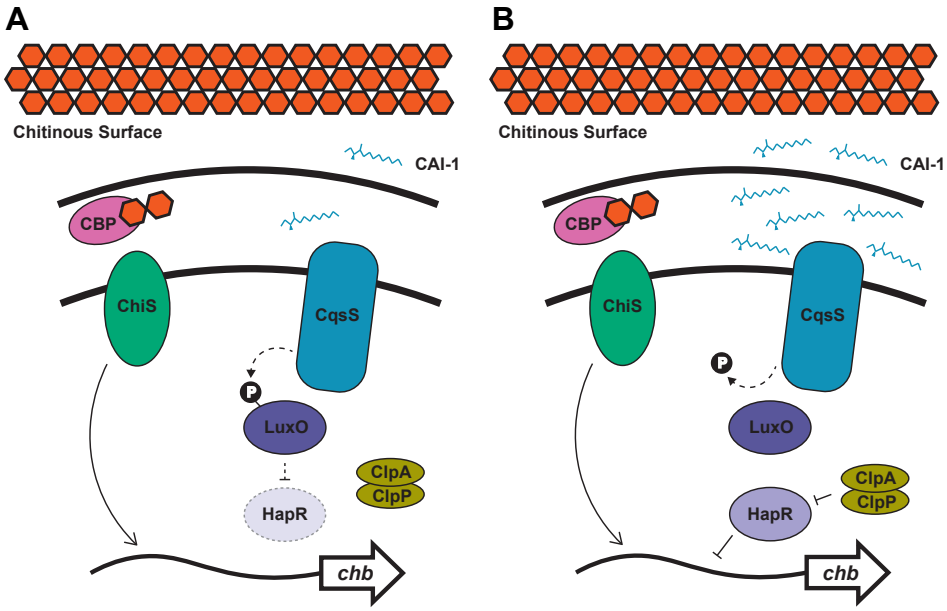

Figure 5. *Model of quorum sensing regulation of chitobiose utilization genes in V. cholerae*. When *V. cholerae* grows on a chitinous surface, the periplasmic chitin binding protein (CBP) binds to chitin oligomers. This de-represses ChiS, which can then activate expression of the chitobiose utilization operon (*chb*). **A**) At low CAI-1 concentrations, the CqsS sensor indirectly promotes LuxO phosphoylation, which indirectly blocks HapR expression. In this state, P_{chb} is maximally expressed. **B**) At high CAI-1 concentrations, the CqsS sensor indirectly dephosphorylates LuxO, which results in activation of HapR expression. HapR then exerts a repressive effect on P_{chb} by decreasing expression of this locus ~2-fold in the presence of the ClpAP protease machine. If HapR is not degraded by ClpAP, its repressive effect can result in a ~7-fold decrease in P_{chb} expression.

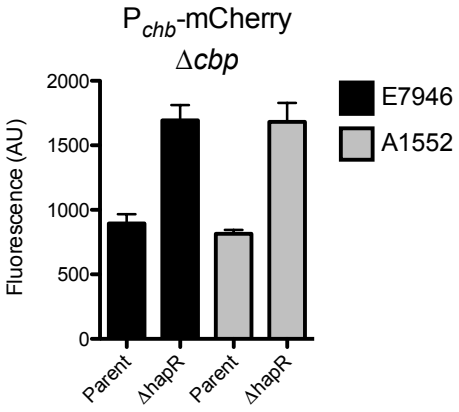

Figure S1. *HapR is a repressor of P_{chb} in V. cholerae E7946 and V. cholerae A1552.* Expression of a P_{chb}-mCherry reporter was determined in the indicated mutant strains. Each respective parent strain contained a P_{chb}-mCherry reporter and a Δ*cbp* mutation to activate ChiS.

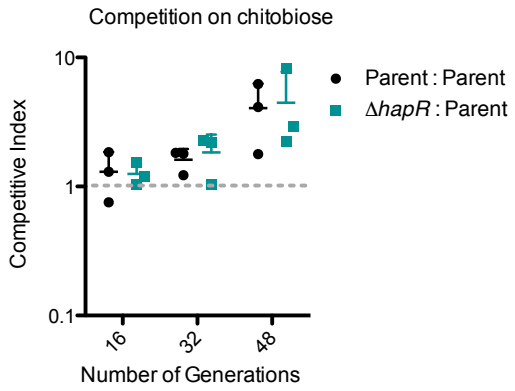

Figure S2. A Δ*hapR mutant does not have a fitness advantage for growth on chitobiose.* The indicated *V. cholerae* strains were mixed and co-cultured in M9 minimal media supplemented with 0.2% chitobiose + 10 μM CAI-1 and grown for the indicated number of generations.

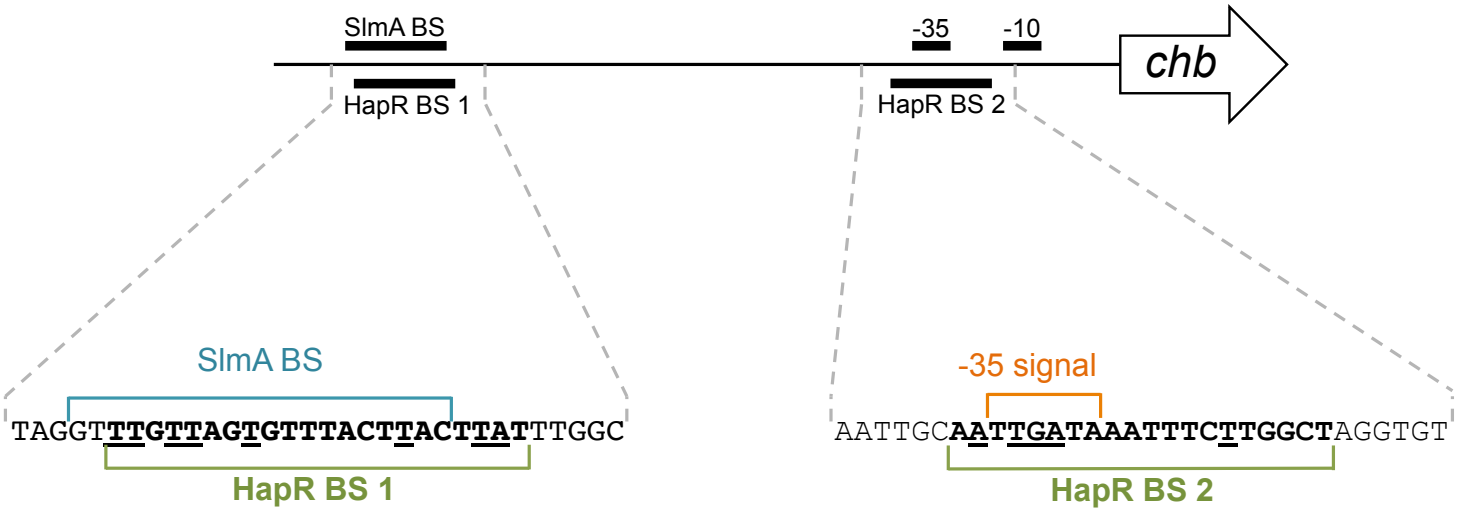

Figure S3. *Sequence of predicted HapR binding sites.* Sequences of the two 32 bp probes used in EMSAs in **Fig. 3C** (for HapR BS 1 and HapR BS 2) are indicated. Predicted HapR binding sites are bolded and bracketed in green; conserved nucleotide residues are underlined. HapR BS 1 was predicted from the SmcR consensus site and HapR BS 2 was predicted from the LuxR consensus site. The SlmA binding site is indicated by the blue bracket and the -35 signal is indicated by the orange bracket.

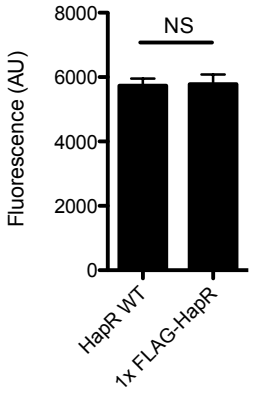

Figure S4. *N-terminally FLAG-tagged HapR is functional for regulation of P_{chb}.* Strains expressing the indicated HapR allele at the native locus were assessed for expression of a P_{chb}-GFP reporter. Both strains also harbored a Δ*cbp* deletion to activate ChiS. Statistical comparisons were made using Student's t-test. NS, not significant.

874 **Table S1.** *Strains used in this study.*
875

Strain Designation (Reference)	Reference in Manuscript	Genotype
SAD 2825/CAK 550 (This Study)	Activator screen strain	Pchb-mCherry @ VC1807, KanR; Pchb-lacZ @ lacZ, SpecR; ChiS @ VCA0692, TmR; Δ3' CBP; pDL1086, CmR CarbR
SAD 2826/CAK 762 (This Study)	ΔclpA counter-screen strain	Pchb-mCherry @ VC1807, KanR; Pchb-lacZ @ lacZ, SpecR; ΔclpA; Δcbp::TmR; pDL1086, CmR CarbR
SAD 1309/CAK 009 (10)	Fig. 1 & 4 Parent; Fig. S4 HapR WT	Pchb-GFP @ lacZ, KanR; Δcbp::SpecR
SAD 2827/CAK 692 (This Study)	Fig. 1 & 4 ΔclpA	Pchb-GFP @ lacZ, KanR; ΔclpA::CarbR; Δcbp::SpecR
SAD 2828/CAK 710 (This Study)	Fig. 1 ΔclpP	Pchb-GFP @ lacZ, KanR; ΔclpP::CarbR; Δcbp::TmR
SAD 2829/CAK 734 (This Study)	Fig. 1 ΔclpAP	Pchb-GFP @ lacZ, KanR; ΔclpA::CarbR; ΔclpP::TmR; Δcbp::SpecR
SAD 2830/CAK 708 (This Study)	Fig. 1 ΔclpS	Pchb-GFP @ lacZ, KanR; ΔclpS::CarbR; Δcbp::TmR
SAD 2831/CAK 712 (This Study)	Fig. 1 ΔclpX	Pchb-GFP @ lacZ, KanR; ΔclpX::CarbR; Δcbp::TmR
SAD 2832/CAK 843 (This Study)	Fig. 1 ΔlonA	Pchb-GFP @ lacZ, KanR; Δlon::TmR; Δcbp::CarbR
SAD 2833/CAK 786 (This Study)	Fig. 1 ΔhapR ΔclpA	Pchb-GFP @ lacZ, KanR; ΔhapR::SpecR; ΔclpA::CarbR; Δcbp::TmR
SAD 2834/CAK 665 (This Study)	Fig. 1 ΔhapR	Pchb-GFP @ lacZ, KanR; ΔhapR::SpecR; Δcbp::CarbR
SAD 2835/CAK 1492 (This Study)	Fig. 2 Parent	Pchb-mCherry @ lacZ, KanR; Pconst2-GFP @ VCA0692, SpecR
SAD 2836/CAK 1505 (This Study)	Fig. 2 ΔhapR	Pchb-mCherry @ lacZ, KanR; Pconst2-GFP @ VCA0692, SpecR; ΔhapR::CmR
SAD 2837/CAK 1498 (This Study)	Fig. 2 Δcbp & Fig. S1 E7946 Parent	Pchb-mCherry @ lacZ, KanR; Pconst2-GFP @ VCA0692, SpecR; Δcbp::TmR
SAD 2838/CAK 1502 (This Study)	Fig. 2 ΔhapR Δcbp & Fig. S1 E7946 ΔhapR	Pchb-mCherry @ lacZ, KanR; Pconst2-GFP @ VCA0692, SpecR; ΔhapR::CmR; Δcbp::TmR
SAD 2839/CAK 869 (This Study)	Fig. 3 ChIP strain and Fig. S4 1x FLAG-HapR	Pchb-GFP @ lacZ, KanR; 1x FLAG-HapR; Δcbp::TmR
SAD 2840/CAK 663 (This Study)	Fig. 4 ΔluxO	Pchb-GFP @ lacZ, KanR; ΔluxO::SpecR; Δcbp::CarbR
SAD 2841/CAK 886 (This Study)	Fig. 4 luxO^{D47E}	Pchb-GFP @ lacZ, KanR; LuxO D47E; Δcbp::SpecR
SAD 2842/CAK 917 (This Study)	Fig. 4 ΔluxS	Pchb-GFP @ lacZ, KanR; ΔluxS::CmR; Δcbp::SpecR
SAD 2843/CAK 915 (This Study)	Fig. 4 ΔcqsA	Pchb-GFP @ lacZ, KanR; ΔcqsA::TmR; Δcbp::SpecR
SAD 2844/CAK 1504 (This Study)	Fig. 4 ΔcqsA ΔhapR	Pchb-GFP @ lacZ, KanR; ΔcqsA::TmR; ΔhapR::CmR; Δcbp::SpecR
SAD 2845/CAK 1506 (This Study)	Fig. S1 A1552 Parent	V. cholerae A1552 Pconst2-GFP @ VCA0692, SpecR; Pchb-mCherry @ lacZ, KanR; Δcbp::TmR
SAD 2846/CAK 1510 (This Study)	Fig. S1 A1552 ΔhapR	V. cholerae A1552 Pconst2-GFP @ VCA0692, SpecR; Pchb-mCherry @ lacZ, KanR; ΔhapR::CmR; Δcbp::TmR
SAD 2847/CAK 942 (This Study)	Fig. S2 WT lacZ+	ΔVC1807::CmR; ΔVC0995
SAD 2848/CAK 944 (This Study)	Fig. S2 WT ΔlacZ	ΔlacZ::SpecR; ΔVC1807::CmR; ΔVC0995

SAD 2849/CAK 1026 (This Study)	Fig. S2 ΔhapR ΔlacZ	ΔlacZ::SpecR; ΔVC1807::CmR; ΔVC0995; ΔhapR::TmR
JDN 71 (This Study)	Fig. 3B, 3C purified HapR	*E. coli* BL21(DE3) harboring pET28b-6XHis-HapR, KanR

876
877

878 **Table S2.** *Primers used in this study.*
879

Pimers for Reporter Constructs		
Primer	**Sequence**	**Description**
ABD 332	GGCTGAACGTGGTTGTCGAAAATGAC	Δ*lacZ* F1 (Up Arm)
BBC 219	GTTTATTTTTGTCGACTGTACAGCGTTTAAATAGAGGTCGATATTGACCC	Δ*lacZ* R1 (Up Arm)
ABD 342	ATTTTTCAGTTGGCCTACAATGCTTTCC	ΔVC1807 F1 (Up Arm)
BBC 719	CACCATACCCACGCCGAAACAAGGATTTTGAATTAAACGTTTCATTAGTC	ΔVC1807 R1 (Up Arm)
BBC 218	CGCTGTACAGTCGACAAAAATAAAC	Kan^R F (Middle Arm)
BBC 262	TACCGAGGACGCGAAGCTG	Kan^R R (Middle Arm)
BBC 266	CAGCTTCGCGTCCTCGGTAGAATAAAGCAATCCGCAAGCG	P_{chb} F (Middle Arm)
BBC 267	CCCGGGATCCTGTGTGAAATTGAGTTGCTTTCATTTCACTAATGG	P_{chb} R (Middle Arm)
BBC 732	ctcaagccgaggagtaaagaagAGTTGCTTTCATTTCACTAATGG	P_{chb} fuse to *lacZ* R (Middle Arm)
BBC 252	CAATTTCACACAGGATCCCGGGAGGAGGTAACGTAATGCGTAAAGGAGAAGAAC	GFP F (Middle Arm)
BBC 254	tgtaggctggagctgcttcTTAGTTGTATAGTTCATCCATGCC	GFP R (Middle Arm)
BBC 1356	TTGTTTCGGCGTGGGTATGGTGCGCTGTACAGTCGACAAAAATAAAC	mCherry F (Middle Arm)
BBC 206	tgtaggctggagctgcttcttacttgtacagctcgtccatg	mCherry R (Middle Arm)
ABD 785	CTTCTTTACTCCTCGGCTTGAG	P_{chb} stitch to *lacZ* F (Down Arm)
ABD 255	gaagcagctccagcctacaCCACAATAAGCCAGAGAGCCTTAAG	Δ*lacZ* F2 (Down Arm)
ABD 256	CCCAAATACGGCAACTTGGCG	Δ*lacZ* R2 (Down Arm)
ABD 341	gaagcagctccagcctacaTAGTCGAAAATAAAAAAAAGAGGCTCGCCTC	ΔVC1807 F2 (Down Arm)
ABD 345	CTTGCTAACCGTTGGTGTTACCAGC	ΔVC1807 R2 (Down Arm)
BBC 3083	tggataactttacgggcatgcataaggctcgtataatatattcagggagaccacaacggtttccctctacaaataatttt gtttaactttCAATTTCACACAGGATCCCGGG	P_{const2} F
BBC 3082	ttatacgagccttatgcatgcccgtaaagttatccagcaaccactcatagacctagggcagcagatagggacgacgt ggtgttagctgtgCTCATTAGGCACCCCAGGC	P_{const2} R
Primers for SOE deletion, FLAG fusions, and point mutants		
Primer	**Sequence**	**Description**
BBC 742	attccggggatccgtcgacCTGCAGTTCagaagcagctccagcctaca	MiniFRT F
BBC 743	tgtaggctggagctgcttctGAACTGCAGgtcgacggatccccggaat	MiniFRT R
ABD 123	ATTCCGGGGATCCGTCGAC	Kan^R, $Spec^R$, $Carb^R$, Cm^R or Tm^R cassette F
ABD 124	TGTAGGCTGGAGCTGCTTC	Kan^R, $Spec^R$, $Carb^R$, Cm^R or Tm^R cassette R
ABD 796	TTAGAATCTGCGCCAGAAGCG	Δcbp F1 (Up Arm)
ABD 797	gtcgacggatccccggaatCATAGCTGTTCCTTACTAGTTGC	Δcbp R1 (Up Arm)
BBC 920	gtcgacggatccccggaatGCTCATCAGGTCGTCAGCC	Δ3'cbp R1 (Up Arm)

ABD 798	gaagcagctccagcctacaGTACTGGATCTGAAACCAGTTAAG	∆cbp F2 (Down Arm)
ABD 799	GTATTGCGGAATGACCAGCATG	∆cbp R2 (Down Arm)
BBC 2755	TTACCCCTAAGTCGGCGAGC	∆VC0995 F1 (Up Arm)
BBC 2756	gtcgacggatccccggaatAATATTCACCTTAAGTTCCCCC	∆VC0995 R1 (Up Arm)
BBC 2757	gaagcagctccagcctacaCTGCCTTAATCGAGTTTAAACCC	∆VC0995 F2 (Down Arm)
BBC 2758	GCACCACGATAGCAATAAGC	∆VC0995 R2 (Down Arm)
CAK 407	GCTACGCACTGCCAAATTACC	∆clpA or ∆clpS F1 (Up Arm)
CAK 408	gtcgacggatccccggaatAAGCATAAGGCCTCCTTAAGGAAC	∆clpA R1 (Up Arm)
CAK 409	gaagcagctccagcctacaCACTAGACATCTCACAATACGC	∆clpA F2 (Down Arm)
CAK 410	CCGCTAACATCTCAGGACTG	∆clpA or ∆clpS R2 (Down Arm)
CKP 449	TGCTCGGTTTTGATCCGTTC	∆clpP or ∆clpX F1 (Up Arm)
CKP 450	gtcgacggatccccggaatGGGCGACATTGCATTTTTTTC	∆clpP R1 (Up Arm)
CKP 451	gaagcagctccagcctacaGGCGAGTAAGCTCGTAATTG	∆clpP F2 (Down Arm)
CKP 454	GTCAAACTAGAAACCAGCGC	∆clpP or ∆clpX R2 (Down Arm)
CKP 447	gtcgacggatccccggaatTTTACTCATGACACTTCAATATTTG	∆clpS R1 (Up Arm)
CKP 448	gaagcagctccagcctacaCAAGCTTAAACTTGCCGGGC	∆clpS F2 (Down Arm)
CKP 452	gtcgacggatccccggaatGTCTGTCATTCGCTAACCTC	∆clpX R1 (Up Arm)
CKP 453	gaagcagctccagcctacaGCGGAGTAATCTCAAGCAAC	∆clpX F2 (Down Arm)
CKP 489	TTGACGCTCTGAAAGCAGAAG	∆lonA F1 (Up Arm)
CKP 490	gtcgacggatccccggaatCAAGTTCATATTTTTCTCTCTTCCG	∆lonA R1 (Up Arm)
CKP 491	gaagcagctccagcctacaGATGCATAGCAAAAATAAGTAAATC	∆lonA F2 (Down Arm)
CKP 492	CGAAGAATTATAAGTGCAAAGGC	∆lonA R2 (Down Arm)
BBC 422	ACGTTCAATAACCAGAATGTTGG	∆hapR F1 (Up Arm)
BBC 423	gtcgacggatccccggaatTTTTCGATTGATGCGTCCATAG	∆hapR R1 (Up Arm)
CKP 511	GTCtttgtcatcgtcatccttataatcCATAGGGGTATATCCTTGCC	1x FLAG-HapR R1 (Up Arm)
BBC 408	gaagcagctccagcctacaAACTAGTTTCTTGGGCAGCACAA	∆hapR F2 (Down Arm)
CKP 510	ATGgattataaggatgacgatgacaaaGACGCATCAATCGAAAAACG	1x FLAG-HapR F2 (Down Arm)
BBC 409	GTTCATAATGATTTCCTTGGTGCC	∆hapR R2 (Down Arm)
BBC 374	TGGCAAAAAGCGAGAGAAGAAG	∆luxO F1 (Up Arm)
BBC 375	gtcgacggatccccggaatCATGAGGACATATTTTGTTTTCTGC	∆luxO R1 (Up Arm)
CKP 519	TCATATCTGGCAAACGTAAcTCCAGCAGGATTAAGTCAGG	luxO^{D47E} R1 (Up Arm)
BBC 376	gaagcagctccagcctacaTAAGCGATGAGAGAATGGATCAAC	∆luxO F2 (Down

		Arm)
CKP 518	TGACTTAATCCTGCTGGAgTTACGTTTGCCAGATATGACG	luxO^{D47E} F2 (Down Arm)
BBC 377	TCACACCCGAATTTCCATCATGC	ΔluxO R2 (Down Arm)
CKP 554	GTCTCTTAGCCGAGGTACTG	ΔcqsA F1 (Up Arm)
CKP 555	gtcgacggatccccggaatCTTGTTCATCGCAATATATCCTAG	ΔcqsA R1 (Up Arm)
CKP 556	gaagcagctccagcctacaTTTCGTTAAATGCATAAATAACAAAAAC	ΔcqsA F2 (Down Arm)
CKP 557	AGTTGGAACCACTTCTTGTC	ΔcqsA R2 (Down Arm)
CKP 549	TACAACTGCTTGGCACGC	ΔluxS F1 (Up Arm)
CKP 550	gtcgacggatccccggaatTGGCATTTCCTTTCTCCC	ΔluxS R1 (Up Arm)
CKP 551	gaagcagctccagcctacaCACTAAGTCGGTTCTGTAAACG	ΔluxS F2 (Down Arm)
CKP 552	TTCTTAGCGTGATCAATTGC	ΔluxS R2 (Down Arm)
ABD 334	AGTGCTCCGGACTCTTTGCTCTG	ΔlacZ F1 (Up Arm)
ABD 254	gtcgacggatccccggaatCATCCCTCAAGCCGAGGAGTAAAG	ΔlacZ R1 (Up Arm)
ABD 255	gaagcagctccagcctacaCCACAATAAGCCAGAGAGCCTTAAG	ΔlacZ F2 (Down Arm)
ABD 256	CCCAAATACGGCAACTTGGCG	ΔlacZ R2 (Down Arm)
ABD 725	GAAGCAGCTCCAGCCTACA	Detect F for all deletions
BBC 082	gtcgacggatccccggaatCATAACTTACACCTTACTCACCCAG	Δcbp detect R
CAK 411	TTGTTTGGTGCGATTATTGG	ΔclpA detect R
CKP 464	TTGGCAGAACATCTTTGATC	ΔclpP detect R
CKP 463	AAAGTATCCAGCTCACGGCG	ΔclpS detect R
CKP 465	CCATGTGTGGATAGACAACC	ΔclpX detect R
CKP 493	CAGTGCCACTTGGTCACCTG	ΔlonA detect R
BBC 410	TAAATGGGGCTTGGAGAATTTAG	ΔhapR detect R
BBC 1911	CGTAATCAAACTGCGAAAGTG	ΔluxO detect R
CKP 558	AATTCGTAACTCTGAGCATG	ΔcqsA detect R
CKP 553	TGGACCACGAACCTTAAACG	ΔluxS detect R
BBC 2759	TTGTCAGAAAGCGTTTCTGC	ΔVC0995 detect R
ABD 399	AACTGATGGCAGAAAAAGCCACTCAG	ΔlacZ detect R
BBC 993	ttgattataaggatgacgatgac	1x FLAG detect F
ABD 846	CATAAACATGTTTCTGATCAGCAG	1x FLAG HapR detect R
BBC 380	GCCAATAGAATGAGTCTATTGGCTG	luxO^{D47E} detect F
CKP 520	TCATATCTGGCAAACGTAgc	luxO^{D47E} detect R
Primers for EMSA probes		
Primer	**Sequence**	**Description**
BBC 744	cagcttcgcgtcctcggtaCGCAAATATAACTCAGGCAAAG	P_{chb} F
CKP 072	cccgggatcctgtgtgaaattgCTTTGGCAGGAGTAAGAAAACACCTAG	P_{chb} R
CKP 865	TAAGCAAACTGTAGCGTAGAAG	P_{clpP} F
CKP 866	TGCATTTTTTTCTTGGTAGC	P_{clpP} R
CKP 504	GCCAAATAAGTAAGTAAACACTAACAAACCTA	HapR BS 1 F
CKP 505	TAGGTTTGTTAGTGTTTACTTACTTATTTGGC	HapR BS 1 R
CKP 506	AATTGCAATTGATAAATTTCTTGGCTAGGTGT	HapR BS 2 F
CKP 507	ACACCTAGCCAAGAAATTTATCAATTGCAATT	HapR BS 2 R
Primers for qPCR		
Primer	**Sequence**	**Description**

BBC 989	GCATCTAGGTTTTGACGTTTTTAACG	P_{chb} amplify F
BBC 990	AACACTCTCCAAGACCTACCTC	P_{chb} amplify R
ABD 132	CTGTCTCAAGCCGGTTACAA	rpoB amplify F
ABD 133	TTTCTACCAGTGCAGAGATGC	rpoB amplify R
CKP 865	TAAGCAAACTGTAGCGTAGAAG	P_{clpP} amplify F
CKP 867	TCGTATGAACGCTCACCACG	P_{clpP} amplify R
Primers for purification vector		
Primer	**Sequence**	**Description**
JDN 92	agcagcggcctggtgccgcgcggcagcCatatggacgcatcaatcgaaaaa	Cloning 6X-His HapR into pET28b vector via IDA, F
JDN 93	tcagtggtggtggtggtggtgCTCGAGctagttcttatagatacacagcatattgagg	Cloning 6X-His HapR into pET28b vector via IDA, R
JDN 22	CTCGAGcaccaccaccacca	Amplify pET28b vector backbone for IDA, F
JDN 23	atGgctgccgcgcggcacca	Amplify pET28b vector backbone for IDA, R

880